JOURNAL OF THEORETICAL
AND APPLIED MECHANICS
4, **37**, 1999

A PROCESS OF GYROSCOPE MOTION CONTROL IN AN AUTONOMOUS SYSTEM OF TARGET DETECTION AND TRACKING

Zbigniew Koruba

Faculty of Mechanical Engineering, Kielce Technical University

e-mail: ksmzko@eden.tu.kielce.pl

A control algorithm of a three-degree-of-freedom gyroscope axis motion emerging from a solution to the inverse problem of dynamic is presented in the paper. A complete system of non-linear differential equations represents the motion of axis of a gimballed gyroscope (i.e. mounted in the Cardan joint), including both the inertial parameters of all elements and resisting forces acting in joint bearings. The effect of the following factors: initial conditions choice, disturbances, as well as non-linearity, on precision of the gyro-axis required motion realisation is presented. Optimal parameters of the control algorithm correcting the gyro-axis motion are determined, as well.

Key words: gyroscope, control, inverse problem of dynamics

1. Introduction

More and more autonomy has been required nowadays in target acquisition and tracking or laser target sensing performed by modern target detection and tracking devices being usually driven by a free gyroscope.

Therefore, there arises a strong need for exploring the possibilities of extending the range of gyroscope application, especially at high angles of gyroscope axis deflection in the space scanning phase. Ways of determination of the required control moments acting upon gyroscope gimbals in the phases of both target detecting and tracking should be explored, as well, and dynamic effects occurring at the target interception instant should be analysed. The problem of interaction between the required platform (eg, launcher, rocket board or unmanned aerial vehicle) motion and realisation of the required motions of the gyroscope axis (hereinafter, for the sake of simplicity, we will use the term "gyro-axis") is also very important. Parameters of this interaction should be optimised in the way ensuring that undesired dynamical effects will be minimised and no resonance couplings will occur.

In the present contribution the control algorithm for gyro-axis motion in both phases of space scanning and target tracking has been constructed basing on the solution to the inverse problem of dynamic (Latała and Osiecki, 1997; Koruba, 1997). The modified Golubencev method has been applied by Dubiel (1986) to optimisation of parameters of the control algorithm correcting the realised motion according to the required gyro-axis motion.

Notations

J_0, J_K	–	principal moments of inertia the gyroscope rotor (gyrowheel)
$J_{Bx1}, J_{By1}, J_{Bz1}$	–	principal moments of inertia of the inner gimbal
$J_{Cx2}, J_{Cy2}, J_{Cz2}$	–	principal moments of inertia of the outer gimbal
m_K	–	gyrowheel mass
r_0	–	distance between the gyrowheel mass centre and the point 0, at which the gimbal axes intersect
$\boldsymbol{M}_C$	–	vector of the resultant moment due to platform acting upon the outer gimbal, $\boldsymbol{M}_C = [M_{Cx2}, M_{Cy2}, M_{Cz2}]$
$\boldsymbol{M}_B$	–	vector of the resultant moment due to outer gimbal acting upon the inner gimbal, $\boldsymbol{M}_B = [M_{Bx2}, M_{By2}, M_{Bz2}]$
$\boldsymbol{M}_K$	–	vector of the resultant moment due to the outer gimbal acting upon the gyrowheel, $\boldsymbol{M}_K = [M_{Kx1}, M_{Ky1}, M_{Kz1}]$
M_{rK}, M_{rB}	–	friction moments in gimbal bearings
M_{rC}	–	air drag moment due to gyrowheel rotation
$\boldsymbol{\omega}$	–	vector of platform angular velocity (kinematic excitation), $\boldsymbol{\omega} = [\omega_X, \omega_Y, \omega_Z]$
ϑ, ψ	–	angles of nutation and precession of gimbals (determining the gyro-axis position)
Φ	–	angle of rotation about the longitudinal axis
$\dot{\vartheta}, \dot{\psi}$	–	angular velocities of nutation and precession of the gyro-axis

$\dot{\Phi}$	–	angular velocity of the gyrowheel rotating about the longitudinal axis (gyrowheel spin)
$\vartheta_z \psi_z$	–	specified angles determining the gyro-axis position in the scanning phase
$\vartheta_s \psi_s$	–	specified angles determining the gyro-axis position in the target tracking phase
$\vartheta_c \psi_c$	–	angles determining the target position
η_b, η_c	–	friction coefficients in gimbal bearings
M_b, M_c	–	control moments in the program-following control of the inner gimbal
M_c	–	control moments in the program-following control of the outer gimbal
$\Delta M_b, \Delta M_c$	–	correcting moments the in program-following control of gimbals
U_b^p, U_c^p	–	control moments in the program-following control of the gyro-axis in the scanning phase
U_b^s, U_c^s	–	control moments in the program-following control of the gyro-axis in the target tracking phase
$\Pi(t_0, tw)$	–	rectangular pulse acting within the time interval $t \in [t_0, t_w]$, $\Pi(t_0, t_w) = H(t - t_0) - H(t - t_w)$
$\Pi(t_0, tw)$	–	rectangular pulse acting within the time interval $t \in [t_s, t_k]$, $\Pi(t_s, t_k) = H(t - t_s) - H(t - t_k)$
$H(\cdot)$	–	Heaviside distribution
t_0	–	scanning start instant
t_w	–	target detection instant
t_s	–	target tracking time
t_k	–	target tracking (illuminating) end
a	–	specified parameter of the Archimedean spiral
v, v_1	–	angular velocities of the gyrowheel in following the specified surfaces
Θ	–	amplitude of angular deflection of the gyrowheel in the required motion
δ_0	–	angle determining the viewfield of the scanning-tracking device
δ	–	trace of the state matrix $\mathbf{A}$
$k_b, k_c, h_b.h_c$	–	amplification coefficients of the correcting moments.

2. Equations of gyro-axis motion

Fig.1 shows a scheme of gimballed gyroscope (mounted in the Cardan joint). The gyrowheel K is mounted by means of bearings in the inner gimbal B, which, in turn, is mounted in the outer gimbal in the same way. Usually, the mass centre of gyrowheel lies at the point, at which the axes of joint bearings intersect (case I), there are, however, the designs, in which it is not true (case II). The outer gimbal is mounted by means of bearings on the platform, which may be fixed or moving relative to the inertial frame of reference. In case I the gyroscope answers only to platform rotations, while in case II also to its translations.

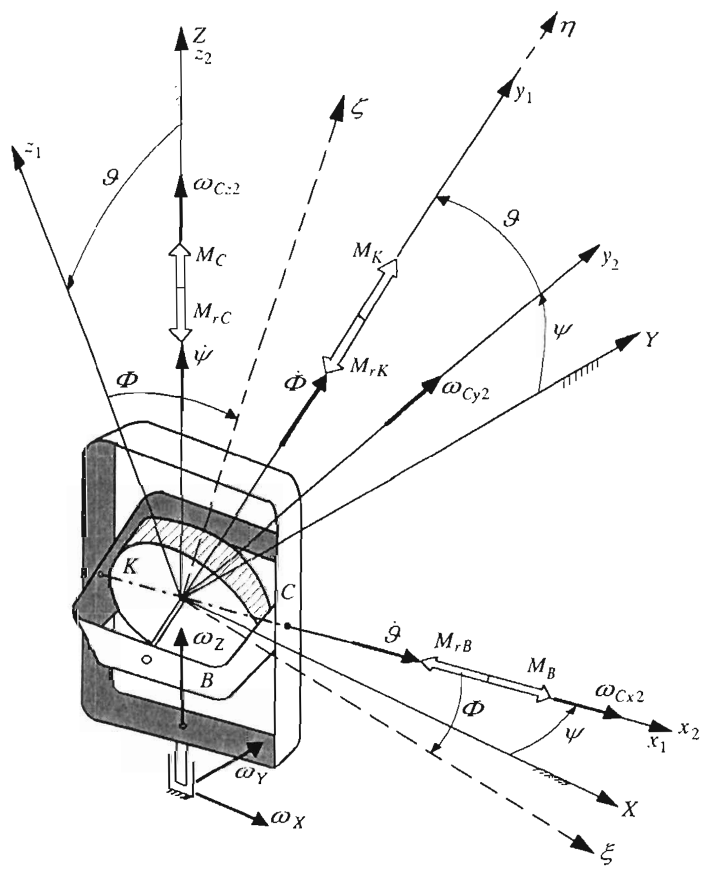

Fig. 1. Scheme of a free gyroscope

The following assumptions were made while deriving the equations of gyro-axis motion:

a) Origin of the Cartesian co-ordinate systems lies at the point of intersection of the Cardan joint axes

b) Axes ξ, η, ζ; x_1, y_1, z_1 and x_2, y_2, z_2 are the principal axes of inertia of the rotor and inner and outer gimbals, respectively

c) Gyro-axis rotates about the movable axes fixed to a corresponding solid (i.e., gyrowheel, inner and outer gimbals, respectively)

d) Gyroscope is axisymmetrical

e) Angular displacements of the platform are also considered

f) Friction moments in inner and outer gimbals are of the viscotic type.

The equations of gyro-axis motion derived using the Lagrange equations of the second kind (Latała and Osiecki, 1997) read

$$
\begin{aligned}
&J_{Ky1}\frac{d(\omega_{By1}+\dot{\Phi})}{dt} = M_{Ky1} - M_{rK}\\
&J_{Bx1}\frac{d(\omega_{Bx1}}{dt} + (J_{Bz1} - J_{By1})\omega_{By1}\omega_{Bz1} + J^{*}_{Kx1}\frac{d\omega_{Bx1}}{dt} + J_K\omega_{By1}\omega_{Bz1} +\\
&-J_0(\omega_{By1}+\dot{\Phi}) = M_{Bx1} - M_{rB} - r_0 m_K g\cos\vartheta\\
&\Big[J_{Bz1}\frac{d(\omega_{Bz1}}{dt} + (J_{By1} - J_{Bx1})\omega_{Bx1}\omega_{By1} + J_K\frac{d\omega_{Bz1}}{dt} + J_0(\omega_{By1}+\dot{\Phi})\omega_{Bx1} +\\
&-J_K\omega_{Bx1}\omega_{By1}\Big]\cos\vartheta + J_{Cz2}\frac{d\omega_{Cz2}}{dt} + (J_{Cy2} - J_{Cx2})\omega_{Cx2}\omega_{Cy2} - M_{Cz2} +\\
&+M_{rC} + \Big[J_{By1}\frac{d\omega_{By1}}{dt} + (J_{Bx1} - J_{Bz1})\omega_{Bx1}\omega_{Bz1} + M_{Ky1} - M_{rK}\Big]\sin\vartheta = 0
\end{aligned}
\tag{2.1}
$$

where

$$
\begin{aligned}
\omega_{Cx2} &= \omega_X\cos\psi + \omega_Y\sin\psi & \omega_{Bx1} &= \dot{\vartheta} + \omega_{Cx2}\\
\omega_{Cy2} &= -\omega_X\sin\psi + \omega_Y\cos\psi & \omega_{By1} &= \omega_{Cy2}\cos\psi + \omega_{Cz2}\sin\psi\\
\omega_{Cz2} &= \dot{\psi} + \omega_Z & \omega_{Bz1} &= -\omega_{Cy2}\sin\psi + \omega_{Cz2}\cos\psi
\end{aligned}
$$

while ϑ, ψ are the generalized coordinates.

For the sake of simplicity we assume that the moment M_K driving the gyrowheel is equal to the resisting moment M_{rK} in the bearings, in which the gyrowheel is mounted, i.e., we have

$$\frac{d(\dot{\Phi}+\dot{\psi}\sin\vartheta)}{dt}=0 \Rightarrow \dot{\Phi}+\dot{\psi}\sin\vartheta=n=\text{const}$$

while at $\dot{\Phi} \gg \dot{\psi}$ it is often assumed that $\dot{\Phi} \approx n$.

By neglecting the moments of inertia of gimbals and assuming that the platform does not rotate, i.e. $\omega_X=\omega_Y=\omega_Z=0$, we arrive at the following form of equations of the gyro- axis motion

$$\begin{aligned}
\frac{d^2\vartheta}{d\tau^2}&=-b_b\frac{d\vartheta}{d\tau}-\frac{1}{2}\Big(\frac{d\psi}{d\tau}\Big)^2\sin 2\vartheta+\frac{d\psi}{d\tau}\cos\vartheta+c_bM_b+\Delta M_b\\
\frac{d^2\psi}{d\tau^2}\cos^2\vartheta&=-b_c\frac{d\psi}{d\tau}+\frac{d\vartheta}{d\tau}\frac{d\psi}{d\tau}\sin 2\vartheta-\frac{d\vartheta}{d\tau}\cos\vartheta+c_cM_c+\Delta M_c
\end{aligned} \tag{2.2}$$

where

$$b_b=\frac{\eta_b}{J_K\Omega} \qquad b_c=\frac{\eta_c}{J_K\Omega} \qquad c_b=c_c=\frac{1}{J_{bK}\Omega^2}$$

$$\Omega=\frac{J_0n}{J_K} \qquad \tau=t\Omega$$

3. Gyro-axis motion control

For the control purposes we preset the required signals, denoted as $\vartheta_z(t),\psi_z(t)$ in the phase of space scanning and $\vartheta_s(t),\psi_s(t)$ in the phase of target tracking. The control problem consists in determination of the time-courses of control moments $M_b(t),M_c(t)$ which will ensure that the gyro-axis will follow the trajectory determined by the angles $\vartheta_z(t),\psi_z(t)$ and $\vartheta_s(t),\psi_s(t)$. Let us put these moments in the form

$$\begin{aligned}
M_b&=\Pi(t_0,t_w)U_b^p+\Pi(t_s,t_k)U_b^s\\
M_c&=\Pi(t_0,t_w)U_c^p+\Pi(t_s,t_k)U_c^s
\end{aligned} \tag{3.1}$$

By rewriting the formulae for the specified angles so as they assume the same form for both the phases, i.e., scanning and tracking

$$\begin{aligned}
\vartheta^*&=\Pi(t_0,t_w)\vartheta_z+\Pi(t_w,t_k)\vartheta_s\\
\psi^*&=\Pi(t_0,t_w)\psi_z+\Pi(t_w,t_k)\psi_s
\end{aligned} \tag{3.2}$$

and after solving the inverse problem of dynamics (Latała and Osiecki, 1997), we can determine the control moments $M_b(t), M_c(t)$ in the form

$$
\begin{aligned}
M_b &= \frac{1}{c_b}\Big[\frac{d^2\vartheta^*}{d\tau^2} + b_b\frac{d\vartheta^*}{d\tau} + \frac{1}{2}\Big(\frac{d\psi^*}{d\tau}\Big)^2 \sin 2\vartheta^* - \frac{d\psi^*}{d\tau}\cos 2\vartheta^*\Big] \\
M_c &= \frac{1}{c_c}\Big[\frac{d^2\psi^*}{d\tau^2}\cos^2\vartheta^* + b_c\frac{d\psi^*}{d\tau} + \frac{d\vartheta^*}{d\tau}\frac{d\psi^*}{d\tau}\sin 2\vartheta^* + \frac{d\vartheta^*}{d\tau}\cos 2\vartheta^*\Big]
\end{aligned}
\tag{3.3}
$$

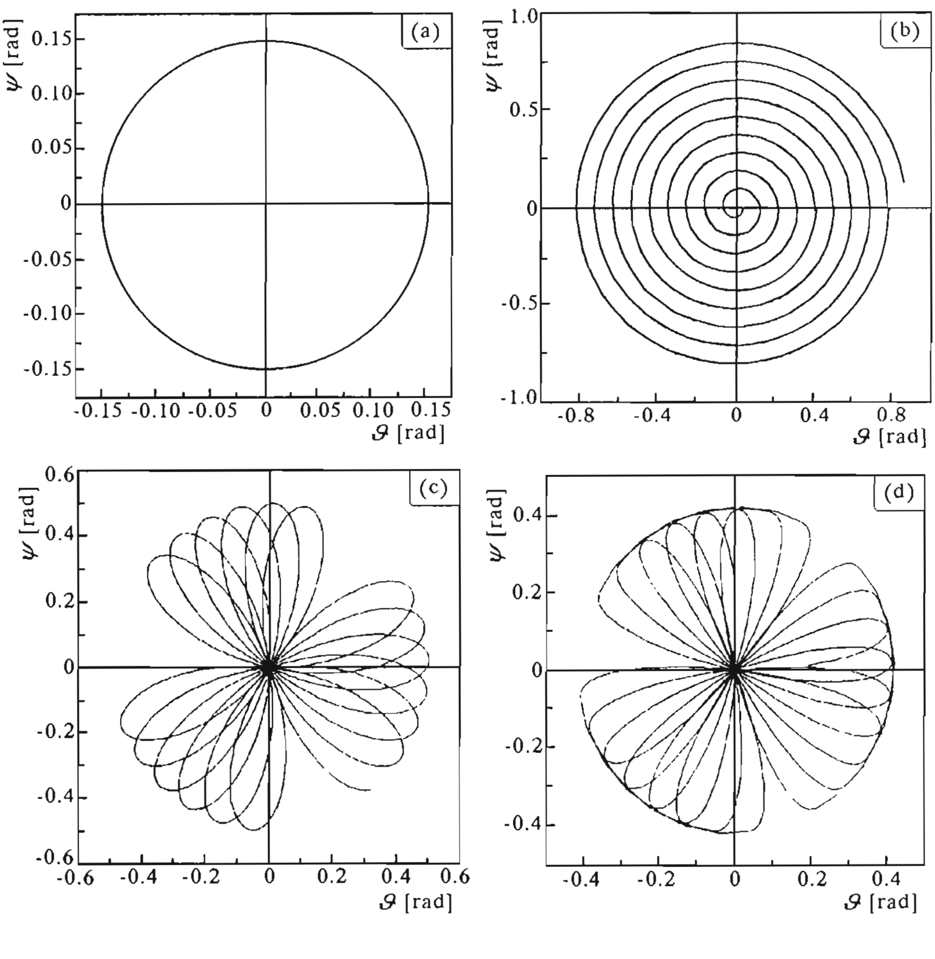

Fig. 2.

Consider the following problem: let the gyro-axis generate the lateral surface of a circular cone (Fig.2a). We require that its motion be

$$\begin{aligned} &\vartheta_z(t) = \Theta \sin(vt) && \psi_z(t) = \Theta \cos(vt) \\ &\frac{d\vartheta_z}{dt} = \Theta v \cos(vt) && \frac{d\psi_z}{dt} = -\Theta v \sin(vt) \\ &\frac{d^2\vartheta_z}{dt^2} = -\Theta v^2 \sin(vt) && \frac{d^2\psi_z}{dt^2} = -\Theta v^2 \cos(vt) \end{aligned} \tag{3.4}$$

In the case when the gyro-axis follows the Achimedean spiral (Fig.2b) we have

$$\begin{aligned} &\vartheta_z(t) = avt \sin(vt) && \psi_z(t) = bvt \cos(vt) \\ &\frac{d\vartheta_z}{dt} = av \sin(vt) + av^2 t \cos(vt) && \frac{d\psi_z}{dt} = bv \cos(vt) - bv^2 t \sin(vt) \\ &\frac{d^2\vartheta_z}{dt^2} = 2av^2 \cos(vt) - av^3 t \sin(vt) && \frac{d^2\psi_z}{dt^2} = -2bv^2 \sin(vt) - bv^3 t \cos(vt) \end{aligned} \tag{3.5}$$

When we require that the giro-axis move along an n-loop rose (Fig.2c) the following set of equations is true

$$\begin{aligned} \vartheta_z(t) &= \Theta \sin(v_1 t) \cos(vt) \\ \psi_z(t) &= \Theta \sin(v_1 t) \sin(vt) \\ \frac{d\vartheta_z}{dt} &= \Theta v_1 \cos(v_1 t) \cos(vt) - \Theta v \sin(v_1 t) \sin(vt) \\ \frac{d\psi_z}{dt} &= \Theta v_1 \cos(v_1 t) \sin(vt) + \Theta v \sin(v_1 t) \cos(vt) \\ \frac{d^2\vartheta_z}{dt^2} &= -\Theta(v^2 + v_1^2) \sin(v_1 t) \cos(vt) - 2\Theta v v_1 \cos(v_1 t) \sin(vt) \\ \frac{d^2\psi_z}{dt^2} &= -\Theta(v^2 + v_1^2) \sin(v_1 t) \sin(vt) + 2\Theta v v_1 \cos(v_1 t) \cos(vt) \end{aligned} \tag{3.6}$$

The case when the gyro-axis moves along a modified n-loop rose (rys.2d) is also very interesting. We arrive at

$$\vartheta_z(t) = \Theta[\sin(v_1 t) + 0.2 \sin(3v_1 t) + 0.04 \sin(5v_1 t)] \cos(vt)$$

$$\psi_z(t) = \Theta[\sin(v_1 t) + 0.2 \sin(3v_1 t) + 0.04 \sin(5v_1 t)] \sin(vt)$$

$$
\begin{aligned}
\frac{d\vartheta_z}{dt} &= \Theta v_1[\cos(v_1 t) + 0.6\cos(3v_1 t) + 0.2\cos(5v_1 t)]\cos(vt) + \\
&\quad -\Theta v[\sin(v_1 t) + 0.2\sin(3v_1 t) + 0.04\sin(5v_1 t)]\sin(vt) \\
\frac{d\psi_z}{dt} &= \Theta v_1[\cos(v_1 t) + 0.6\cos(3v_1 t) + 0.2\cos(5v_1 t)]\sin(vt) + \\
&\quad +\Theta v[\sin(v_1 t) + 0.2\sin(3v_1 t) + 0.04\sin(5v_1 t)]\cos(vt) \\
\frac{d^2\vartheta_z}{dt^2} &= -\Theta(v^2 + v_1^2)[2\sin(v_1 t) + 2\sin(3v_1 t) + 1.04\sin(5v_1 t)]\cos(vt) + \\
&\quad -2\Theta v v_1[\cos(v_1 t) + 0.6\cos(3v_1 t) + 0.2\cos(5v_1 t)]\sin(vt) \\
\frac{d^2\psi_z}{dt^2} &= -\Theta(v^2 + v_1^2)[2\sin(v_1 t) + 2\sin(3v_1 t) + 1.04\sin(5v_1 t)]\sin(vt) + \\
&\quad +2\Theta v v_1[\cos(v_1 t) + 0.6\cos(3v_1 t) + 0.2\cos(5v_1 t)]\cos(vt)
\end{aligned} \tag{3.7}
$$

Substituting Eqs (3.4) ÷ (3.7) into Eqs (3.3) we determine the time-dependent control moments $U_b^p(t), U_c^p(t)$, ensuring the required giro-axis motion to be realised is the scanning phase. For a circular cone the control moments read

$$
\begin{aligned}
U_b^p &= \Theta v(1 - v)\sin(vt) + b_b\Theta v\cos(vt) \\
U_c^p &= \Theta v(1 - v)\cos(vt) - b_c\Theta v\sin(vt)
\end{aligned} \tag{3.8}
$$

In the same way we determine the control moments $U_b^s(t), U_c^s(t)$ ensuring the gyro-axis motion in the target tracking phase, but in this case the values of angles ϑ_c, ψ_c determining the target position, as well as their first and second time derivatives have to be known a priori. The information about parameters specifying the target motion can be acquired using devices of different type; e.g., optoelectronic (passive target coordinator in rocket missiles), radar, laser (active or semi-active target coordinators) or wave-guides mounted on the gyro-axis. The device axis pointing at the target may determine the line of sight (LOS).

When the axis coincides with the LOS the target tracking phase begins. At this instant the radiation energy emitted (or reflected) by the target is detected by the image analysis system, i.e., the target has already entered the viewfield of the tracking system.

When denoting the angles the gyro-axis makes with the LOS as follows

$$
\begin{aligned}
e_\vartheta &= \vartheta_z - \vartheta_c & \qquad e_\psi &= \psi_z - \psi_c \\
\dot{e}_\vartheta &= \frac{d\vartheta_z}{dt} - \frac{d\vartheta_c}{dt} & \qquad \dot{e}_\psi &= \frac{d\psi_z}{dt} - \frac{d\psi_c}{dt}
\end{aligned}
\tag{3.9}
$$

$$
e = \sqrt{e_\vartheta^2 + e_\psi^2} \tag{3.10}
$$

then the relation

$$
e \leqslant \delta_0 \tag{3.11}
$$

defines the condition for target interception.

Let us assume that neither the amplitudes of angular deviations from the required gyro-axis trajectory nor the kinematic excitation due to platform exceed 0.1. We assume additionally that angular errors in realisation of the required motion are small, i.e.

$$
\Delta\vartheta = \vartheta - \vartheta^* \ll 1 \qquad \Delta\psi = \psi - \psi^* \ll 1 \tag{3.12}
$$

With a sufficient accuracy Eqs (2.2) can be linearised with respect to the required trajectory. Therefore, they read

$$
\begin{aligned}
\frac{d^2\Delta\vartheta}{d\tau^2} &= -b_b\frac{d\Delta\vartheta}{d\tau} + \frac{d\Delta\psi}{d\tau} - \frac{d\overline{\omega}_x}{d\tau} + \Delta M_b \\
\frac{d^2\Delta\psi}{d\tau^2} &= -b_c\frac{d\Delta\psi}{d\tau} - \frac{d\Delta\vartheta}{d\tau} - \overline{\omega}_x + \Delta M_c
\end{aligned}
\tag{3.13}
$$

where

$$
\begin{aligned}
\Delta M_b &= k_b\Delta\vartheta + h_b\frac{d\Delta\vartheta}{dt} & \qquad \overline{\omega}_x &= \frac{\omega_x}{J_K} \\
\Delta M_c &= k_c\Delta\vartheta + h_c\frac{d\Delta\vartheta}{dt}
\end{aligned}
\tag{3.14}
$$

Fig.3 shows the way of control of a free gyroscope motion in an autonomous system of target detection and tracking (or laser target sensing).

4. Selection of optimal correcting moments

In the case when magnitudes of the friction forces in gimbals bearings are small the kinematic excitations due to the platform may cause substantial

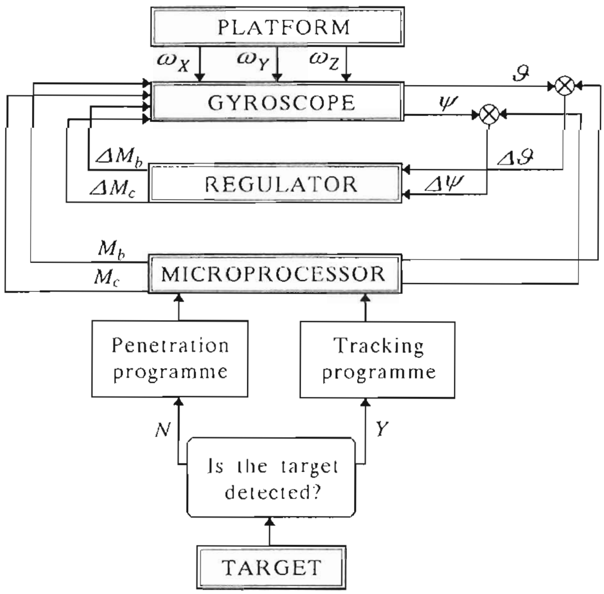
PLATFORM
ω_X
ω_Y
ω_Z
GYROSCOPE
ϑ
ψ
ΔM_b
ΔM_c
REGULATOR
$\Delta\vartheta$
$\Delta\psi$
M_b
M_c
MICROPROCESSOR
Penetration programme
Tracking programme
N
Y
Is the target detected?
TARGET

Fig. 3.

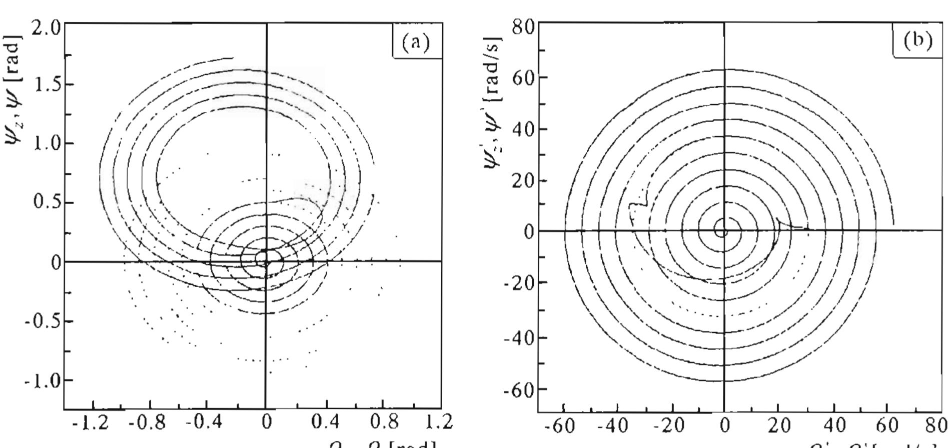
(a)
ψ_z, ψ [rad]
ϑ_z, ϑ [rad]
(b)
ψ_z', ψ' [rad/s]
ϑ_z', ϑ' [rad/s]

Fig. 4.

deviations from the required motion (see Fig.4). To avoid this disadvantageous effect, a feed-back realised by a simple PD regulator represented by Eqs $(3.14)_{2,3}$ should be introduced to the control system.

Substituting Eqs $(3.14)_{2,3}$ into Eqs (3.13) and putting $\omega_x = 0$ we obtain

$$
\begin{aligned}
\frac{d^2\Delta\vartheta}{d\tau^2} &= \overline{k}_b\Delta\vartheta + \overline{h}_b\frac{d\Delta\vartheta}{d\tau} + \frac{d\Delta\psi}{d\tau} + \Delta M_b \\
\frac{d^2\Delta\psi}{d\tau^2} &= \overline{k}_c\Delta\psi + \overline{h}_c\frac{d\Delta\psi}{d\tau} - \frac{d\Delta\vartheta}{d\tau} + \Delta M_c
\end{aligned}
\tag{4.1}
$$

where

$$
\overline{k}_b = \frac{k_b}{J_K\Omega^2} \qquad \overline{k}_c = \frac{k_c}{J_K\Omega^2}
$$

$$
\overline{h}_b = \frac{h_b}{J_K\Omega} - b_b \qquad \overline{h}_c = \frac{h_c}{J_K\Omega} - b_c
$$

Let us rewrite the equations of the gyro-axis motion (4.1) in the vector form

$$
\boldsymbol{X}' = \mathbf{A}\boldsymbol{X} \tag{4.2}
$$

where

$$
\boldsymbol{X}' = \frac{d\boldsymbol{X}}{d\tau} \qquad \boldsymbol{X} = \Big[\Delta\vartheta, \frac{d\Delta\vartheta}{d\tau}, \Delta\psi, \frac{d\Delta\psi}{d\tau}\Big]^\top
$$

$$
\mathbf{A} = \left[\begin{array}{cccc} 0 & 1 & 0 & 0 \\ \overline{k}_b & \overline{h}_b & 0 & 1 \\ 0 & 0 & 0 & 1 \\ 0 & -1 & \overline{k}_c & \overline{h}_c \end{array}\right] \tag{4.3}
$$

Let us introduce a new variable

$$
\boldsymbol{x}(\tau) = \boldsymbol{y}(\tau)\mathrm{e}^{\delta(\tau)} \tag{4.4}
$$

at the same time

$$
\delta = \operatorname{tr}\mathbf{A} = \frac{1}{4}(\overline{h}_b + \overline{h}_c) \tag{4.5}
$$

After transformation we have

$$
\boldsymbol{Y}' = \mathbf{B}\boldsymbol{Y} \tag{4.6}
$$

where

$$
\mathbf{B} = \left[\begin{array}{cccc} -\delta & 1 & 0 & 0 \\ \overline{k}_b & \overline{h}_b - \delta & 0 & 1 \\ 0 & 0 & -\delta & 1 \\ 0 & -1 & \overline{k}_c & \overline{h}_c - \delta \end{array}\right] \tag{4.7}
$$

We look for the values of $\overline{k}_b, \overline{k}_c, \overline{h}_b, \overline{h}_c$ for which the characteristic equation has only imaginary roots or they equal to zero.

To this end the coefficients of characteristic equation of $\mathbf{B}$ should be determined in the following way

$$
\begin{aligned}
b_1 &= \operatorname{tr}\mathbf{B} = 0\\
b_2 &= \sum\begin{vmatrix} b_{ii} & b_{ij}\\ b_{ji} & b_{jj}\end{vmatrix} > 0(j>i) \Rightarrow \begin{vmatrix} -\delta & 1\\ \overline{k}_b & \overline{h}_b-\delta\end{vmatrix} + \begin{vmatrix} -\delta & 0\\ 0 & -\delta\end{vmatrix} +\\
&+\begin{vmatrix} -\delta & 1\\ \overline{k}_b & \overline{h}_b-\delta\end{vmatrix} + \begin{vmatrix} \overline{h}_b-\delta & 0\\ 0 & -\delta\end{vmatrix} + \begin{vmatrix} \overline{h}_b-\delta & 1\\ -1 & \overline{h}_c-\delta\end{vmatrix} + \begin{vmatrix} -\delta & 1\\ \overline{k}_c & \overline{h}_c-\delta\end{vmatrix} > 0
\end{aligned}
\tag{4.8}
$$

thus

$$
\overline{k}_b + \overline{k}_c < -\frac{3}{8}(\overline{h}_b+\overline{h}_c)^2 + \frac{7}{16}\overline{h}_b\overline{h}_c + 1 \tag{4.9}
$$

And

$$
\begin{aligned}
b_3 &= \sum\begin{vmatrix} b_{ii} & b_{ij} & b_{ik}\\ b_{ji} & b_{jj} & b_{jk}\\ b_{ki} & b_{kj} & b_{kk}\end{vmatrix} > 0(k>j>i) \Rightarrow \begin{vmatrix} -\delta & 1 & 0\\ \overline{k}_b & \overline{h}_b-\delta & 0\\ 0 & 0 & -\delta\end{vmatrix} +\\
&+\begin{vmatrix} -\delta & 1 & 0\\ \overline{k}_b & \overline{h}_b-\delta & 1\\ 0 & -1 & \overline{h}_c-\delta\end{vmatrix} + \begin{vmatrix} -\delta & 0 & 0\\ 0 & -\delta & 1\\ 0 & \overline{k}_c-\delta & \end{vmatrix} + \begin{vmatrix} \overline{h}_b-\delta & 0 & 1\\ 0 & -\delta & 1\\ -1 & \overline{k}_c & \overline{h}_c-\delta\end{vmatrix} = 0
\end{aligned}
\tag{4.10}
$$

therefore

$$
(4.11)\overline{k}_b = \frac{(\overline{h}_b+\overline{h}_c)[(\overline{h}_c-\overline{h}_b)^2-4]}{4(\overline{h}_c-\overline{h}_b)} + \overline{k}_c \tag{4.11}
$$

And

$$
b_4 = \det\mathbf{B} > 0 \Rightarrow \begin{vmatrix} -\delta & 1 & 0 & 0\\ \overline{k}_b & \overline{h}_b-\delta & 0 & 1\\ 0 & 0 & -\delta & 1\\ 0 & -1 & \overline{k}_c & \overline{h}_c-\delta\end{vmatrix} > 0 \Rightarrow
$$

$$
\begin{aligned}
&\overline{k}_b\overline{k}_c + \frac{1}{16}(\overline{h}_b+\overline{h}_c)\Big[\overline{k}_b(3\overline{h}_c-\overline{h}_b) + \overline{k}_c(3\overline{h}_b-\overline{h}_c) + \overline{h}_b + \overline{h}_c\Big] >\\
&> -\frac{1}{256}(\overline{h}_b+\overline{h}_c)^2(3\overline{h}_b-\overline{h}_c)(3\overline{h}_c-\overline{h}_b)
\end{aligned}
\tag{4.12}
$$

When considering the problem not only Eq (4.11), representing the relation between $\overline{k}_b$ and $\overline{k}_c$ amplification coefficients of the regulator should be taken into account, but also the following, very important condition for maximisation of the absolute value of $\mathbf{A}$ trace

$$|\operatorname{tr}\mathbf{A}| = \left|\frac{1}{4}(\overline{h}_b + \overline{h}_c)\right| = \max \tag{4.13}$$

If we assume that $k_b = k_c$ then we will find the following additional relation between the coefficients $\overline{h}_b, \overline{h}_c$

$$\overline{h}_c = \overline{h}_b \pm 2 \tag{4.14}$$

Finally if the conditions (4.8), (4.9), (4.12) and (4.13), are satisfied then the transient processes occurring in the system (see Eqs (4.1)) will decay rapidly.

5. Numerical results

The following values for the parameters used in the process of gyro-axis motion control in the scanning-tracking system have been taken

- Gyroscope parameters: $J_0 = 2.5 \cdot 10^{-4}\,\mathrm{kg\,m^2}$, $J_K = 5.0 \cdot 10^{-4}\,\mathrm{kg\,m^2}$, $n = 600\,\mathrm{rad/s}$
- Angle determining the viewfield of scanning-tracking system: $\delta_0 = 0.02\,\mathrm{rad}$
- Optimal values correcting moments amplifications: $k_b = k_c = -10$, $\overline{h}_b = -5.32$, $\overline{h}_c = -7.32$
- Angles, which determine the target position have been assumed as follows

$$\vartheta_c = \vartheta_{c0} + \omega_c t \sin(\omega_c t) \qquad \psi_c = \psi_{c0} + \omega_c t \cos(\omega_c t)$$

  where $\vartheta_{c0} = \psi_{c0} = 0.2\,\mathrm{rad}$, $\omega_c = 0.5\,\mathrm{rad/s}$

- Scanning phase was limited to the gyro-axis required motion along the Archimedean spiral (Fig.2b) of the following parameters

$$v = 2\pi\frac{\Theta}{\delta_0} \qquad \Theta = 1\ \mathrm{rad}$$

- *Kinematic excitations due to the platform* have had the form

$$\omega_x = \omega_{x0}\cos(pt) \qquad \omega_y = \omega_{y0}\cos(pt) \qquad \omega_z = \omega_{z0}\cos(pt)$$

  where $\omega_{x0} = \omega_{y0} = \omega_{z0} = 1\,\mathrm{rad/s}$, $p = 5\,\mathrm{rad/s}$ and were of $\Delta t = 0.05\,\mathrm{s}$ duration, arising at the instant $t = 0.5\,\mathrm{s}$.

In Fig.4 ÷ Fig.8 the simulation results are presented. Fig.5a shows the trajectories of required (dotted line) and realised motions, respectively, of the gyro-axis for the initial conditions different from those required, while the angular velocities in this situation are shown in Fig.5b. The effect of non-linearity (see Fig.6) and transient kinematic excitation due to platform (Fig.4) on the precision of the program-following control realisation in the scanning phase can be clearly seen. Fig.7 show the trajectories of gyro-axis and target, respectively, in the process of target detection and tracking with no correcting control employed (Fig.7a) and when applying the correcting signals of optimal parameters (Fig.7b). Fig.8 illustrate the transient processes occurring at the target interception instant, which cannot be clearly seen in Fig.4b and Fig.7a.

6. Conclusions

Basing on the above considerations and the results presented it can be concluded that the following factors affect the precision of realisation of the free gyroscope required motion in a scanning-tracking system.

- **Initial conditions.** When improper values are assumed for the angles determining the initial gyro-axis position the required trajectory will be realised in a wrong region (Fig.5a). While improper initial values assumed for the gyro-axis angular velocities involve transient processes (Fig.5b). These processes decay, however, quickly due to friction in gimbal bearings.

- **Disturbances in terms of kinematic excitations due to the platform.** At a low friction level in gimbal bearings even weak excitations of short duration may cause a substantial deviation from the required trajectory (Fig.4).

- **Amplitudes of the required angular deflections of gyro-axis.** The influence of non-linearity on the precision of the required trajectory realisation is exerted at high values of the amplitudes.

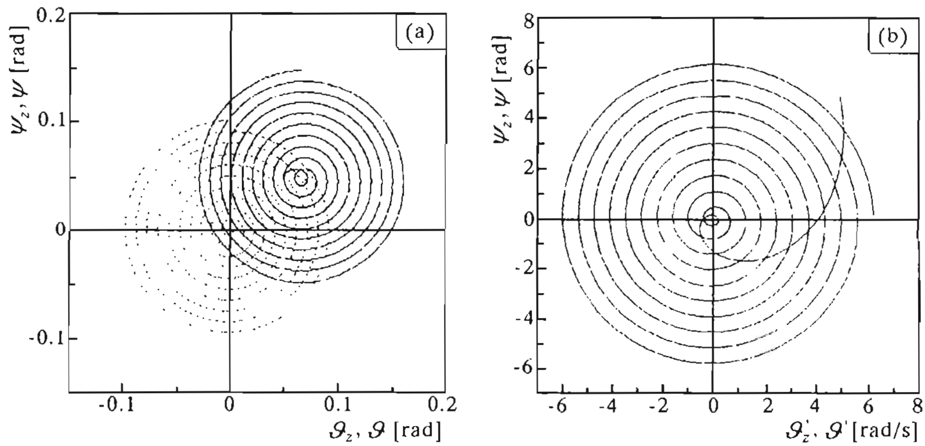
(a)
(b)
0.2
0.1
0
-0.1
-0.1
0
0.1
0.2
8
6
4
2
0
-2
-4
-6
-6
-4
-2
0
2
4
6
8
ψ_z, ψ [rad]
ϑ_z, ϑ [rad]
ϑ_z', ϑ' [rad/s]

Fig. 5.

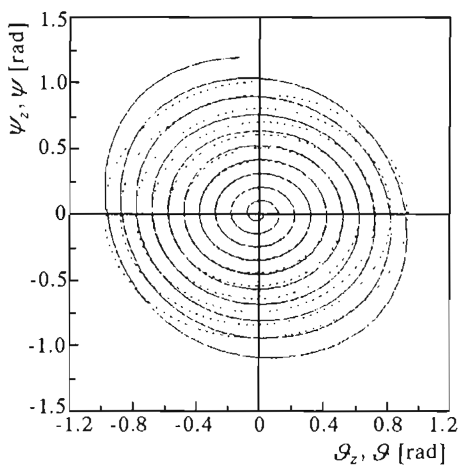
1.5
1.0
0.5
0
-0.5
-1.0
-1.5
-1.2
-0.8
-0.4
0
0.4
0.8
1.2
ψ_z, ψ [rad]
ϑ_z, ϑ [rad]

Fig. 6.

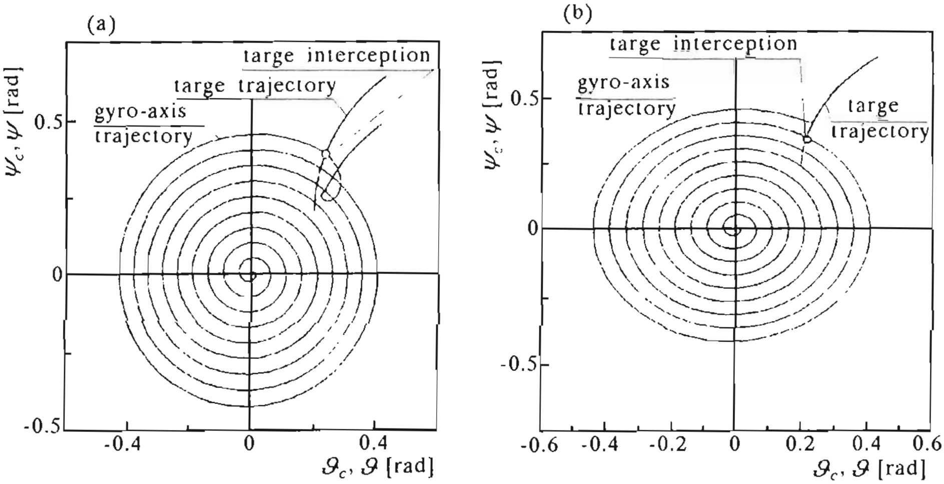

(a)
targe interception
targe trajectory
gyro-axis trajectory
ψ_c, ψ [rad]
0.5
0
-0.5
-0.4
0
0.4
ϑ_c, ϑ [rad]
(b)
targe interception
gyro-axis trajectory
targe trajectory
ψ_c, ψ [rad]
0.5
0
-0.5
-0.6
-0.4
-0.2
0
0.2
0.4
0.6
ϑ_c, ϑ [rad]

Fig. 7.

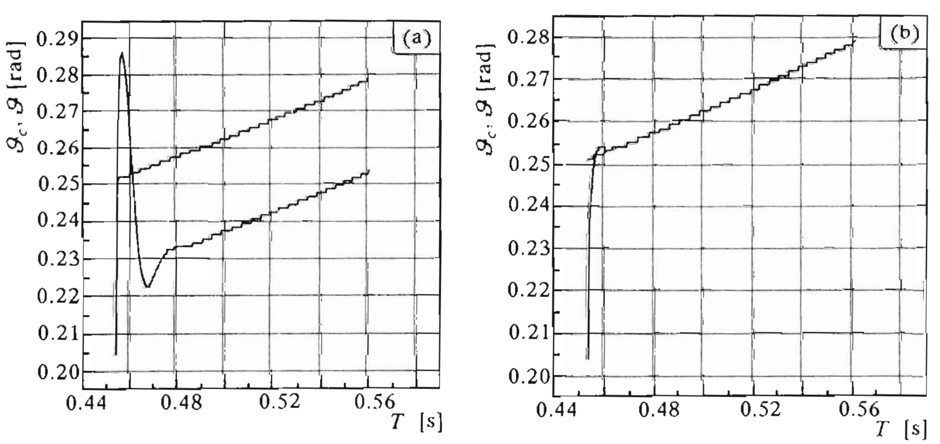

(a)
ϑ_c, ϑ [rad]
0.29
0.28
0.27
0.26
0.25
0.24
0.23
0.22
0.21
0.20
0.44
0.48
0.52
0.56
T [s]
(b)
ϑ_c, ϑ [rad]
0.28
0.27
0.26
0.25
0.24
0.23
0.22
0.21
0.20
0.44
0.48
0.52
0.56
T [s]

Fig. 8.

- **Transient process occurring at the target detection instant.** A rapid change in the control moments may cause the target to leave the viewfield of the tracking system.

Bad influence of the above factors is exerted particularly at a low friction level in gimbal bearings (what, unfortunately is the aim of gyroscope designers). To avoid this influence a stabilising regulator should be introduced into the control system. Optimisation of the regulator parameters performed in the way presented in Section 4 ensures additionally that the transient processes occurring due to disturbances involved by the platform or when changing the phase, will be attenuated rapidly.

The following problems should be also taken into consideration in further research:

- Selection of the optimal scanning program realised by the gyro-axis for minimal time and maximal probability of the target detection, in the cases when it is immovable, movable and non-manoeuvring or movable and manoeuvring, respectively.

- Determination of the optimal values of the platform/gyroscope system parameters ensuring quickest possible attenuation of dynamic effects and avoidance of critical states (resonance).

- Construction of the control algorithm of platform motion, which would ensure most suitable conditions of target tracking and laser target pointing (in the case of unmanned aerial vehicle) or quickest target interception (in the case of homing rocket).

- Offering the possibility of the space scanning phase restarting in case the target leaves the tracking device viewfield.

References

1. Dubiel S., 1986, Liniowe układy mechaniczne o najszybszym tłumieniu, *Mechanika Teoretyczna i Stosowana*, **34**, 3

2. Koruba Z., 1997, Optymalna redukcja drgań układu giroskopowego o trzech stopniach swobody, *Materiały III Szkoły "Metody Aktywne Redukcji Drgań i Hałasu"*, Kraków-Zakopane, 115-120

3. LATAŁA T., OSIECKI J., 1997, Zastosowanie metody zagadnień odwrotnych dynamiki w sterowaniu układów mechanicznych, *Materiały Konferencyjne VI Krajowej Konferencji "Automatyzacja i eksploatacja systemów sterowania"*, Gdynia, 209-216

Sterowanie giroskopem w autonomicznym układzie wykrywania i śledzenia celu

Streszczenie

W pracy przedstawiono wyniki sterowania ruchem osi giroskopu o trzech stopniach swobody, którego program sterowania jest wyznaczany za pomocą tzw. metod odwrotnych dynamiki. Ruch osi giroskopu, zawieszonego na przegubie Cardana, został opisany pełnym układem nieliniowych równań różniczkowych z uwzględnieniem bezwładności wszystkich elementów giroskopu oraz sił oporu w łożyskach przegubu. Pokazano wpływ warunków początkowych, zakłóceń oraz nieliniowości na dokładność realizacji ruchu programowego osi giroskopu. Wyznaczono parametry optymalne sterowań stabilizujących ruch osi giroskopu.

Manuscript received October 1, 1998; accepted for print March 4, 1999